A chaotic spiking oscillator that acts as a filter of spike trains

Seiji Uenohara, Takashi Morie

Graduate School of Life Science and Systems Engineering, Kyushu Institute of Technology
2–4 Hibikino Wakamatsu-ku, Kitakyushu 808–0196, Japan
Email: uenohara-seiji@edu.brain.kyutech.ac.jp

Abstract—We propose a chaotic spiking oscillator model that functions as a filter of spike trains, in which input/output signals are spike pulses. The oscillator receives periodic spike inputs, and the internal state of an oscillator is mapped by a nonlinear function, otherwise the internal state increases with a constant rate. The oscillator outputs a spike pulse when the internal state exceeds a threshold for firing. This model uses the input-spike interval as a bifurcation parameter; that is the input-spike interval changes an attractor of the internal state. If the firing threshold is outside of the range of the internal state determined by the attractor, the oscillator outputs no spike. The oscillator acts as a filter of spike trains by this characteristic. In this study, we show that the oscillator acts as a low pass filter, a band stop filter, and a filter combining both characteristics by changing the firing threshold.

1. Introduction

Among many oscillator models were proposed so far [1, 2, 3, 4], pulse-coupled oscillators transmit information between each other with pulse timing [4]. The oscillators can output periodic and chaotic spike trains, which was implemented by a discrete electronic circuit [5, 6, 7], and by CMOS integrated circuits [8].

In order to express various information by spike patterns, it is necessary to generate various spike patterns including output/non-output of spike pulses. Output/non-output of spikes to the input-spike patterns can be considered as a filter of spike trains.

We propose a chaotic spiking oscillator that functions as a filter of spike trains. Our oscillator outputs a chaotic spike train or no spikes according as the input spike interval. In this study, we investigate the relationship between the period of input-spike trains and the output-spike interval or the firing rate.

2. Mathematical model of the oscillator

Internal state x of the oscillator is expressed as

$$x = \omega t \mod x_{rst}, \tag{1}$$

$$S_{out} = \begin{cases} 1 & \text{if } x = x_{th}, \\ 0 & \text{if } x \neq x_{th}, \end{cases} \tag{2}$$

where ω is the natural frequency, t continuous time, x_{rst} the resetting threshold for the internal state, x_{th} the firing threshold, and S_{out} represents output spikes. Internal state x increases monotonically toward x_{rst} with ω. The oscillator outputs spike S_{out} when x exceeds x_{th}.

It is noted that x is never reset unless x reaches x_{rst} even if the oscillator outputs spike S_{out}. This is a unique feature of the proposed model. When x reaches x_{rst}, x is reset to zero. Internal state x is mapped as

$$x \to f(x) \quad \text{if } S_{in} = 1, \tag{3}$$

where $f(\cdot)$ is the update function of x, and S_{in} represents input spikes.

Figure 1 shows the timing diagram of the updating scheme. When no spikes output, the oscillator outputs spikes with constant period x_{rst}/ω as shown in Fig. 1(a). The update result of x depends on timing because x increases constantly as shown in Fig. 1(b). Firing time of the oscillator is changed by Eq. (3), which varies spike-interval of S_{out}. The range of x is determined by attractors generated by S_{in} and $f(\cdot)$. The attractors determine the filtering characteristics, which is determined by setting x_{th} and x_{rst} individually.

3. Simulation and analysis method

3.1. Simulation method

In order to simplify numerical simulations, we defined a return map of x between input spike timing and the next timing in S_{in}. We conducted numerical simulations, and calculated spike-interval T_{out} of S_{out} using this return map, where T_{out} is defined as the time-interval between adjacent spikes, and time-step is defined by input-spike S_{in}. We assumed the spike width to be negligibly small. In this study, we employed a chaotic neuron model [9] as $f(\cdot)$:

$$f(x) = kx + \alpha/(1 + \exp((x + 0.5)/\epsilon)) + a, \tag{4}$$

where we set $\omega = x_{rst} = \alpha = 1$ and $\epsilon = 0.05$, k and a are treated as parameters in this model.

Internal state x increases by ωT_{in} until it is updated by input-spike S_{in}, where T_{in} is the input-spike interval. Internal state x_{i+1} at time-step $(i + 1)$ is expressed by

$$x_{p,i} = x_i + \omega T_{in} \mod x_{rst}, \tag{5}$$

$$x_{i+1} = f(x_{p,i}), \tag{6}$$

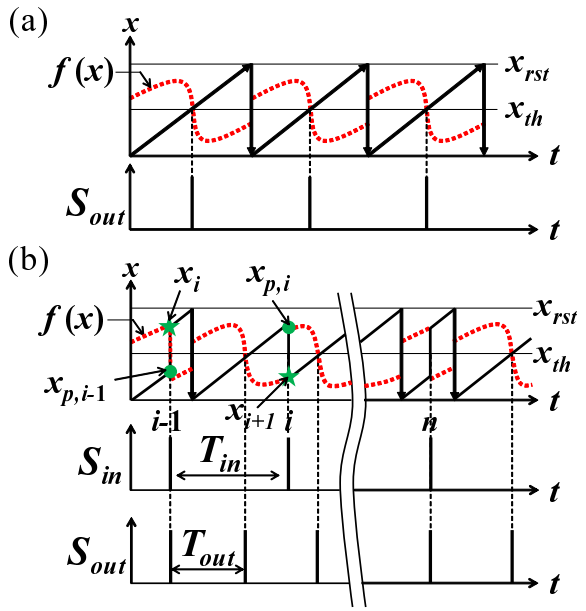

Figure 1: Timing diagram of updating scheme: (a) without spike inputs and (b) for periodic spike inputs.

where $x_{p,i}$ is the internal state just before updating as shown in Fig. 1(b). We calculate T_{out} according to T_{in} and $x_{d,i}$ given by the following equation:

$$x_{d,i} = \begin{cases} x_{th} - x_i & \text{if } x_{th} \geq x_i, \\ x_{th} - x_i + x_{rst} & \text{if } x_{th} < x_i. \end{cases} \quad (7)$$

When $x_{d,i}/\omega \leq T_{in}$, spike S_{out} is outputted because x reaches x_{th} before next spike S_{in} is given. When $x_{d,i}/\omega > T_{in}$, $x_{p,i} < x_{th}$ and $x_{th} \leq x_{i+1}$, S_{out} is outputted at the same timing with S_{in}. When $x_{d,i}/\omega > T_{in}$, $x_{p,i} \geq x_{th}$ and $x_{th} > x_{i+1}$, S_{out} is not outputted.

3.2. Analysis method

We distinguished between periodic spike-trains and chaotic spike-trains using the maximum value $C_{\max}$ of the normalized autocorrelation function $C(q)$ as defined by the following equation.

$$C(q) = \frac{\langle \tilde{T}_j \tilde{T}_{j+q} \rangle}{\langle \tilde{T}_j^2 \rangle}, \quad (8)$$

where j is the index of output-spike S_{out}, T_j is the output-spike interval between j-th and $(j+1)$-th output spikes, $\tilde{T}_q = T_q - \langle T_j \rangle$, and $\langle T_j \rangle$ denotes the long-time average of T_j with respect to j. If the spike-train is periodic, $C_{\max}$ equals unity. For a chaotic spike-train, $C_{\max}$ is smaller than unity. In this analysis, we set $q = 1,000$ and the number of spikes for averaging is 10,000.

4. Numerical simulation results

4.1. Relation between Input and Output-spike intervals

We investigated T_{out} when T_{in} is varied. The first 10,000 input-spikes were assumed to be transition time. We used the following parameters: $k = 0.97$, $a = -0.5$, and $x_{th} = 0.5$.

Figure 2 shows the change of T_{out} and $C_{\max}$ for different T_{in}. Our proposed oscillator exhibits bifurcation phenomena when T_{in} is changed as shown in Fig. 2(a). There are regions where $C_{\max} = 1$ and those where $C_{\max} < 1$ as shown in Fig. 2(b). This result means that the obtained spike-trains contain periodic and chaotic spike-trains. Moreover, output-spike interval T_{out} equals T_{in} in the region of about $0.4 \leq T_{in} \leq 0.7$.

Figure 4 shows time-series of x, $f(x)$, S_{in}, and S_{out}. Although parameters of $f(x)$ are the same in all cases, the ranges of x are different as shown in Fig. 4 when T_{in} is changed because input-spike interval T_{in} is one of the parameters as expressed by Eq. (5).

4.2. Firing rate

We investigated the firing rate for various k, a, x_{th}, and T_{in}, where the firing rate is defined as the ratio of the number of output-spikes m to that of input-spikes n in time-window nT_{in} as shown in Fig. 3. We set here $n = 100$.

Figure 5 shows that firing-rate m/n is small when T_{in} is short (high frequency). Figure 5(c) includes regions where firing-rate m/n equals zero (black regions), which means the oscillator is turned off. We can consider these black regions as *cutoff* regions of a filter. If we set x_{th} at the values indicated by white broken lines in Fig. 5(c), the oscillator acts as the following filters: (1) a low-pass filter, (2) a band-stop filter, and (3) a filter combining both characteristics.

5. Discussion

The input-spike interval T_{in} acts as a bifurcation parameter as shown in Fig. 2(a). The bifurcation diagram in this figure can be scaled by period x_{rst}/ω of the oscillator. Therefore, the resolution of T_{in} can be improved by reducing x_{rst}/ω, which is an advantage when the oscillator is implemented in an electronic circuit. If we represent x in the voltage domain we can control the bifurcation parameter at high resolution without expanding the voltage range. We can observe even a long periodic orbit that has been difficult to observe until now. As with the bifurcation diagram, the firing rate shown in Fig. 5 can also be scaled by x_{rst}/ω. Therefore, the cutoff region of the oscillator can be change by scaling x_{rst}/ω.

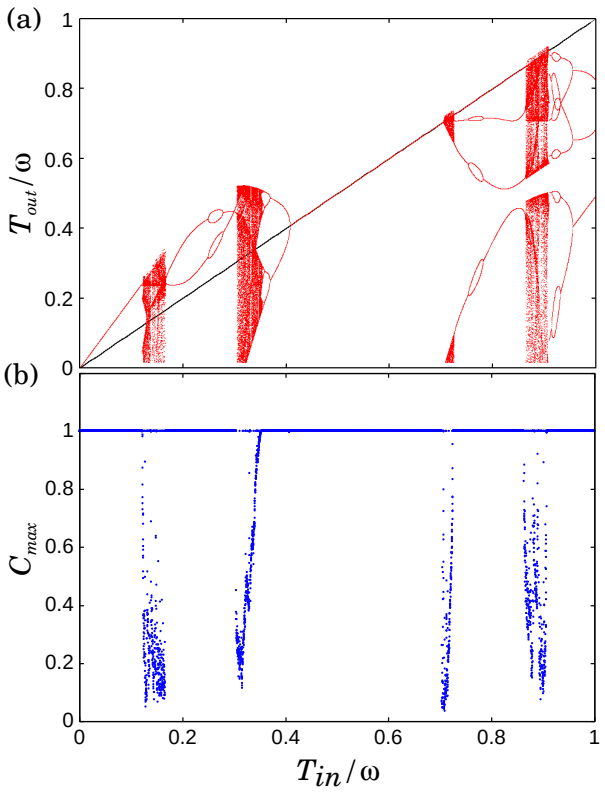

Figure 2: Output-spike interval T_{out} and the maximum value of autocorrelation function C_{max} when T_{in} is changed, where we set $x_{th} = 0.5$: (a) T_{in}/ω vs. T_{out}/ω, and (b) T_{in}/ω vs. C_{max}. The black line represents $T_{in} = T_{out}$.

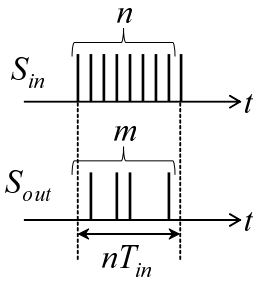

Figure 3: Definition of time-window nT_{in}.

6. Conclusion

We proposed a chaotic spiking oscillator that acts as a filter of spike trains. In numerical simulations, we investigated behaviors of the oscillator when periodic spike-pulses are given. The obtained spike-trains were analyzed by the normalized autocorrelation function.

As a result of numerical simulations, chaotic and periodic spike-trains were included in the obtained spike-trains. The oscillator outputted no spikes according as the value of the input spike interval. This characteristic changes by varying the firing threshold. We showed that the oscillator acts as a low pass filter, a band stop filter, and a filter combining both characteristics by varying the firing threshold.

References

[1] Y. Kuramoto, *Chemical oscillations, waves, and turbulence*. Springer-Verlag (Berlin and New York), 1984.

[2] A. T. Winfree, *The geometry of biological time*. Springer, 2001, vol. 12.

[3] R. Perez and L. Glass, "Bistability, period doubling bifurcations and chaos in a periodically forced oscillator," *Physics Letters A*, vol. 90, no. 9, pp. 441–443, 1982.

[4] R. E. Mirollo and S. H. Strogatz, "Synchronization of pulse-coupled biological oscillators," *SIAM Journal on Applied Mathematics*, vol. 50, no. 6, pp. 1645–1662, 1990.

[5] K. Mitsubori and T. Saito, "Mutually pulse-coupled chaotic circuits by using dependent switched capacitors," *IEEE Trans. Circuits and Systems I: Fundamental Theory and Applications*, vol. 47, no. 10, pp. 1469–1478, 2000.

[6] H. Nakano and T. Saito, "Grouping synchronization in a pulse-coupled network of chaotic spiking oscillators," *IEEE Trans. Neural Networks*, vol. 15, no. 5, pp. 1018–1026, 2004.

[7] Y. Matsuoka, T. Hasegawa, and T. Saito, "Chaotic spike-train with line-like spectrum," *IEICE trans. Fundamentals.*, vol. 92, no. 4, pp. 1142–1147, 2009.

[8] K. Matsuzaka, T. Tohara, K. Nakada, and T. Morie, "Analog CMOS circuit implementation of a pulse-coupled phase oscillator system and observation of synchronization phenomena," *Nonlinear Theory and Its Applications, IEICE*, vol. 3, pp. 180–190, 2012.

[9] K. Aihara, T. Takabe, and M. Toyoda, "Chaotic neural networks," *Physics letters A*, vol. 144, no. 6, pp. 333–340, 1990.

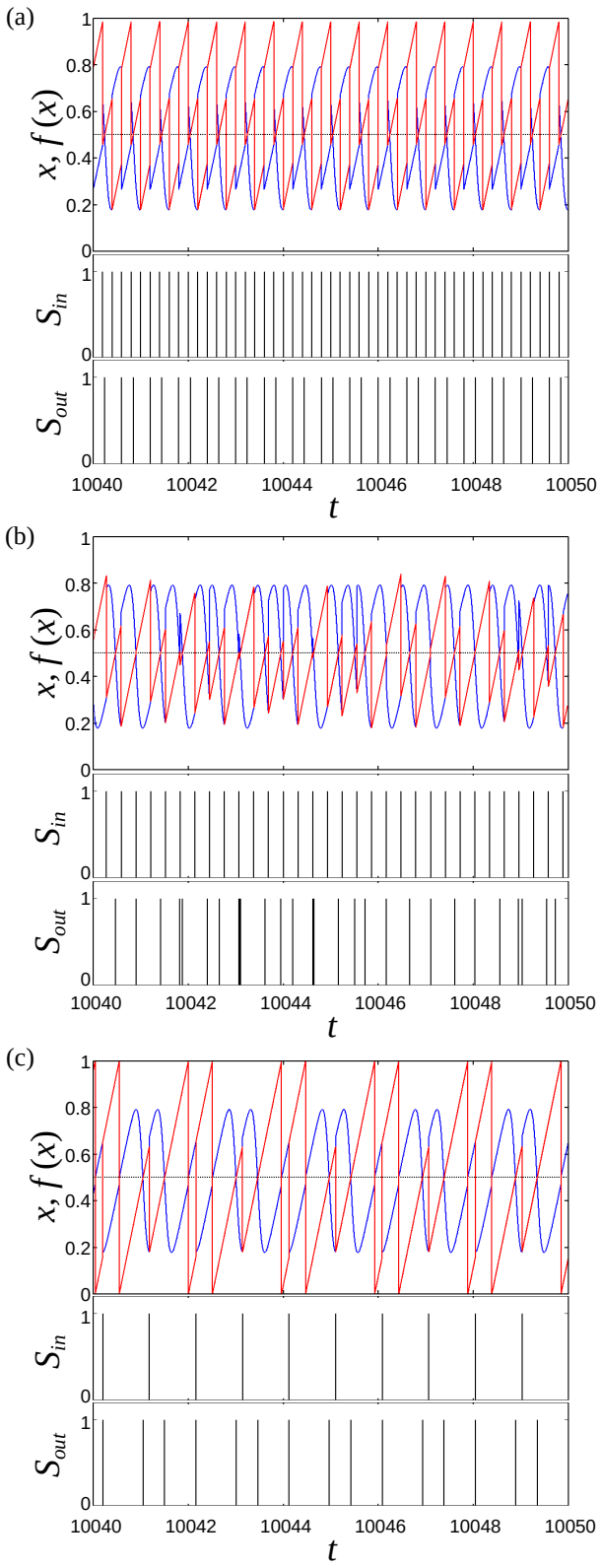

Figure 4: Time-series of state variable x, update function $f(x)$, input-spike S_{in}, and output-spike S_{out} obtained with different spike-interval T_{in}: (a) $T_{in} = 0.2$ (period two), (b) $T_{in} = 0.31$ (chaos), and (c) $T_{in} = 0.98$ (period three). The blue and red lines represent x and $f(x)$, respectively.

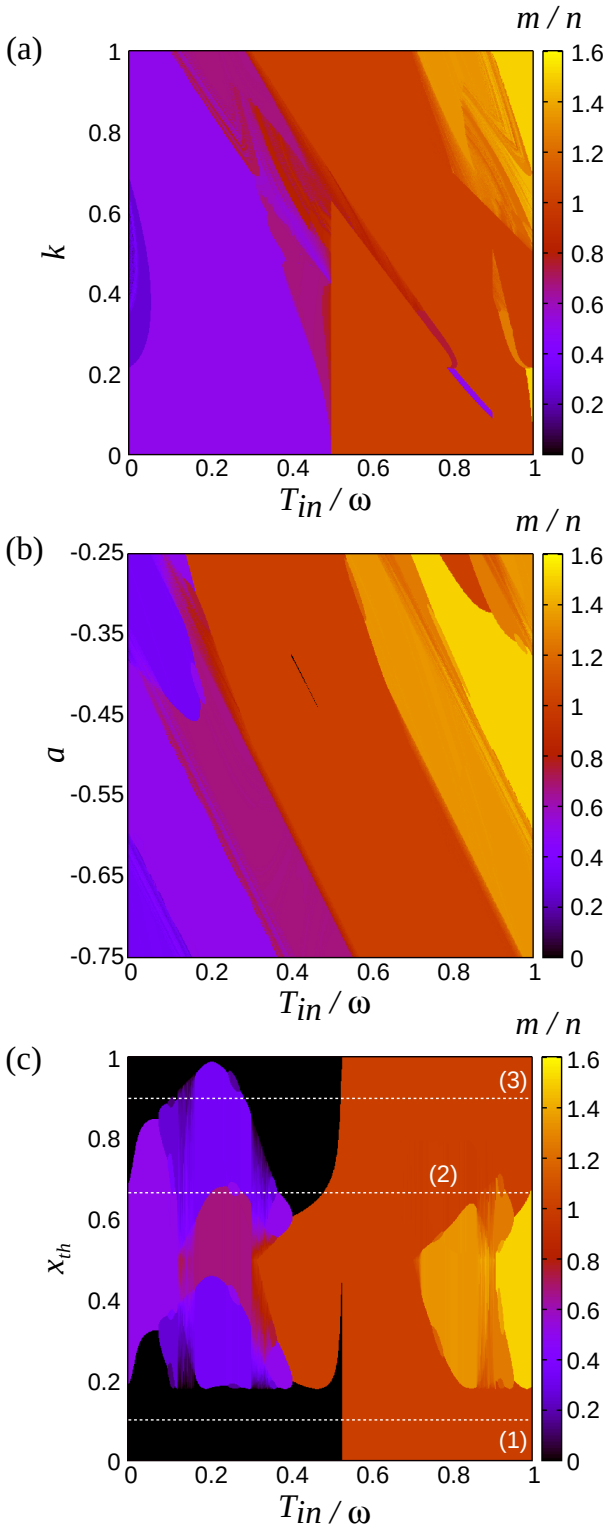

Figure 5: Firing-rate m/n of the oscillator: (a) $\alpha = 1$, $a = -0.5$, and $x_{th} = 0.5$; (b) $k = 0.97$, $\alpha = 1$, and $x_{th} = 0.5$; (c) $k = 0.97$, $\alpha = 1$, and $a = -0.5$. We considered the period $n = [0, 10000]$ as transition time.